Nanotechnology **21** (2010) 265704 (5pp) doi:10.1088/0957-4484/21/26/265704

Luminescence dynamics of Te doped CdS quantum dots at different doping levels

Wenzhi Wu[1,2], **Hongan Ye**[2] **and Xiulin Ruan**[1,3]

[1] School of Mechanical Engineering and the Birck Nanotechnology Center, Purdue University, West Lafayette, IN 47907-2088, USA
[2] School of Electronic Engineering, Heilongjiang University, Harbin 150080, People's Republic of China

E-mail: ruan@purdue.edu

Received 1 December 2009, in final form 20 April 2010
Published 10 June 2010
Online at stacks.iop.org/Nano/21/265704

Abstract

We have examined steady-state and time-resolved luminescence properties of CdS:Te quantum dots (QDs). The transient emission spectra have a red shift along the emission process. Using singular value decomposition and multiexponential decay analysis, the luminescence is found to originate from two distinct and parallel channels: band-edge excitonic emission and trapping state emission. With increasing amount of Te, the emission peaks of the QDs show an obvious red shift. Our experimental results suggest that CdS:Te quantum dots have tunable emission spectra and luminescence lifetimes which may have applications in chemical sensing, high throughput screening and other biotechnological applications.

(Some figures in this article are in colour only in the electronic version)

1. Introduction

Semiconductor nanocrystals or quantum dots (QDs), such as CdS, CdSe, CdTe and ZnSe QDs, have shown great promise for applications in fluorescence image displays [1], light-emitting diodes [2] and solar energy conversion [3] owing to their size-confined and size-tunable electric and optical properties [4]. Some applications, such as biological labeling of brain tumors, prefer a specific dot size to break through the blood–brain barrier (BBB), and also prefer the emission to be in the red or near-infrared band in order to avoid visible biofluorescence from organism multiplexing experiments. Binary compound QDs in the desired size range, however, usually emit in the visible band rather than the red and near-infrared range. One preferential solution to this challenge is to use doped QDs [5, 6], since their emission can be tuned by varying the doping composition when the size is fixed [7]. Also, dopants in QDs may introduce new characteristics such as the cubic-power dependence luminescence and longer lifetime in Cu and Mn doped QDs [8, 9].

One such system that has received considerable attention are the doped CdS QDs [10–12]. Compared with CdTe and CdSe, CdS has a larger band gap (2.58 eV) and a smaller Bohr exciton radius (2.8 nm), which is expected to show a weaker quantum confinement effect and a lower photoluminescence quantum efficiency in a similar size range. By incorporating impurity atoms into CdS QDs, the dominant recombination route can change to the impurity related trapping states [13]. Rogach *et al* [14] showed that the photoluminescence lifetime of CdSe:Te QDs increases with the amount of Te doping, and the recombination of charge carriers trapped by Te impurities occurs on a slower timescale than for bare CdSe QDs. The luminescence dynamics of excitonic and trapping states in doped CdS QDs is not yet clearly understood. Knowledge about how dynamic luminescence properties depend on the amount of doping is essential to synthesize appropriate QDs for biomedical and solar energy applications.

In this work transient luminescence spectroscopy is used to study the luminescence mechanisms in CdS:Te QDs in the visible and near-infrared spectral range. We first report the time-domain luminescence spectra with an emission peak shift in CdS:Te QDs. Using singular value decomposition and biexponential fitting, the luminescence is decomposed into two distinctive components, the origins of which are assigned using a proposed energy level model. We then explain the peak shift in time-resolved spectra at the earlier time delay [15]. The variation of the luminescence properties with the doping level is also reported and discussed.

[3] Author to whom any correspondence should be addressed.

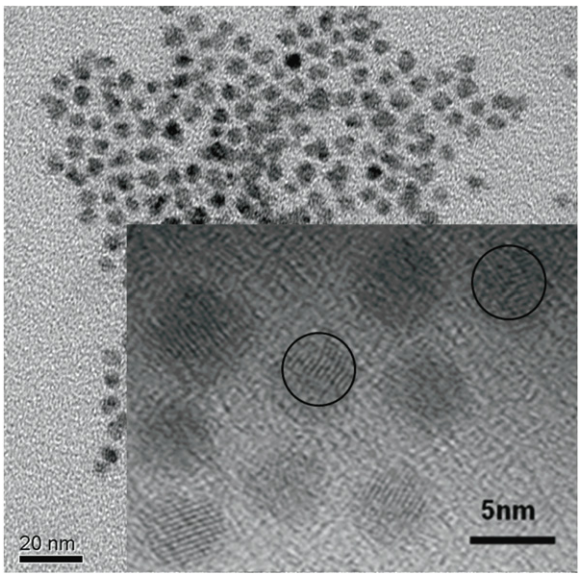

Figure 1. TEM image of CdS:Te:1.1% QDs. Inset: HRTEM of CdS:Te:1.1% QDs. The black circles mark individual QDs, for which the size is about 4.7 nm in the zoom-out image.

2. Experimental details

2.1. Synthesis and preparation of CdS:Te QDs

In the synthesis of CdS:Te QDs, Cd, Te and S solutions are separately prepared. A mixture of CdO (0.496 g), oleic acid (1.63 mmol) and 1-octadecene (18 g) is heated at 320 °C and then lowered to 300 °C to be used as the Cd precursor. Elemental Te and S in trioctylphosphine solvent are then injected into the cadmium precursor. Three CdS:Te QD samples are prepared with varied amounts of Te, where the molar ratio of Te/S is controlled by varying the relative amount of the starting materials. The non-polar QDs and reaction solutions are then injected into methanol which is polar and can separate 1-octadecene/oleic acid and doped nanocrystals. After evaporation of organic solvent the CdS:Te QD powders are deposited. The amount of Te and S in CdS:Te QDs is measured by inductively coupled plasma mass spectroscopy (ICP-MS), and the three CdS:Te QD samples display different Te/S molar ratios: 1.1%, 2.3% and 7.5%.

2.2. Experimental setup for the characterizations

To investigate the effect of Te doping on the luminescence properties of CdS:Te QDs in toluene, we also performed time-resolved luminescence studies under femtosecond laser excitation. A Ti:sapphire regenerative amplifier (1 kHz, Spectra Physics, Spitfire) produces ∼130 fs pulses at 800 nm. The 400 nm femtosecond pulses could also be produced by high-level harmonic generation using a BBO nonlinear crystal. Time-resolved luminescence spectra are measured using a spectrometer (Bruker Optics 250IS/SM) with an intensified charge coupled device (ICCD; IStar740, Andor). The instrument response time τ is 2 ns when scattering femtosecond laser pulses are measured.

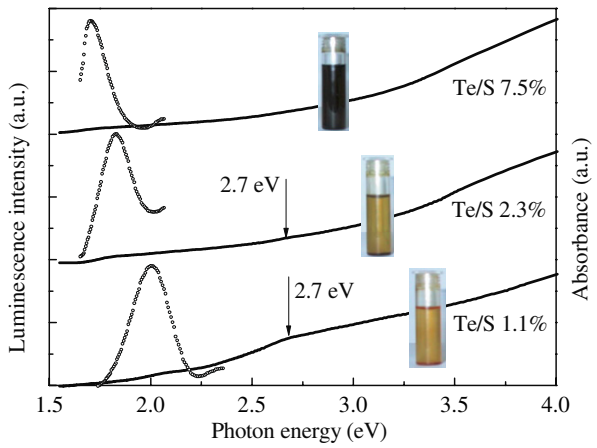

Figure 2. Room-temperature UV–visible absorption (solid lines) and photoluminescence (dotted lines) spectra of CdS:Te QDs with different Te/S molar ratios. Inset: photograph of three CdS:Te QDs in toluene in glass tubes.

3. Results and discussion

3.1. Steady-state absorption and luminescence spectra of CdS:Te QDs

UV–visible absorption spectra are measured on colloidal solutions of the three CdS:Te QD samples with a Shimadzu UV-2550 spectrophotometer. Steady-state photoluminescence (PL) measurements are carried out using an assembled PL setup with a Jobin-Yvon 450 W Xe lamp and TRIAX 180 monochromators, and the data are collected with a photomultiplier tube. The focal length of both monochromators is 0.19 m. The overall spectral resolution of the PL setup is 0.5 nm. The steady-state emission spectra are recorded with fluorimeter (Shimadzu, RF-5000) using a quartz cuvette (10 mm optical path) and Xe lamp excitation at 3.10 eV. High-resolution transmission electron microscopy (HRTEM) measurement is performed with a Tecnai G220 S-Twin microscope operating at a high voltage at 200 kV, where the CdS:Te:1.1% QD samples are prepared by dropping dilute solutions of QDs in toluene on to carbon-coated copper grids. The QDs are spherical and sufficiently monodisperse and well separated with a size distribution of 4.7 ± 0.4 nm, as shown in figure 1. The average size of the sample is determined from the TEM image using Image Pro-Plus software.

The band gap of CdS:Te QDs can be tuned by controlling the Te concentration, and the value is between the band gap of CdTe QDs and CdS QDs of the same size. Figure 2 shows the absorption and PL spectra for different Te concentrations. With the Te content increasing from 1.1% to 7.5%, the emission peak clearly shifts from the red (corresponding to CdS QDs) to the near-infrared band (corresponding to CdTe QDs), as expected. The absorption maximum bands are also slightly shifted from red to near-infrared as denoted by arrows in figure 2. Note that when the Te content is increased from 2.3% to 7.5%, the absorption peak is not distinguishable because of lattice mismatching [16]. The samples also exhibit a large Stokes shift (e.g. 160 nm for CdS:Te:1.1% QDs) between the

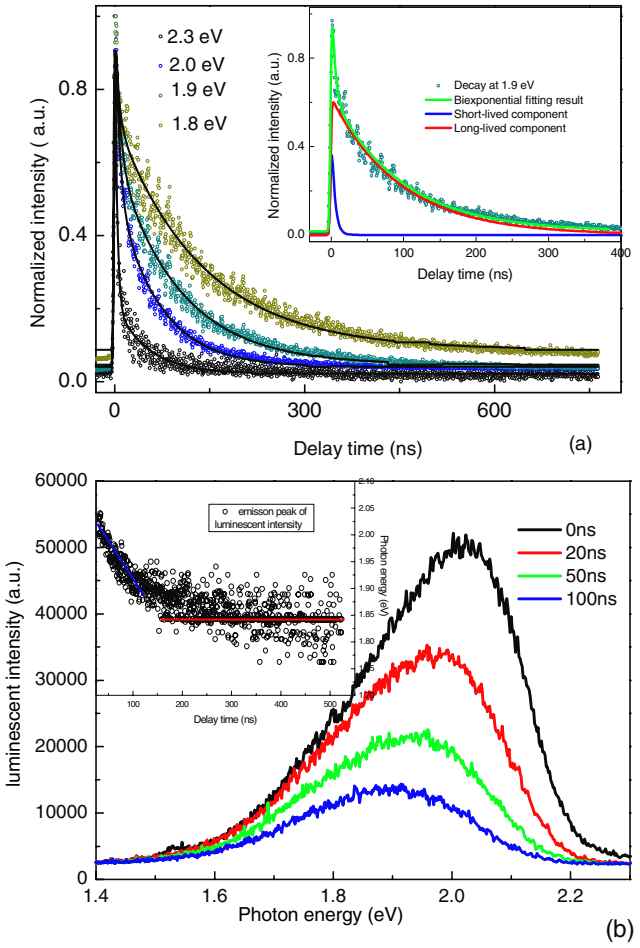

Figure 3. (a) PL decay curves of CdS:Te:1.1% QDs for photon energies of 2.3, 2.0, 1.9 and 1.8 eV, respectively. The solid lines are exponential fitting curves of experimental data. Inset: corresponding experimental result, its biexponential fitting, long-lived component, and short-lived component. (b) Temporal evolution of PL spectra from 0 to 100 ns from top to bottom. Inset: the spectra are shifted vertically and the times are indicated in the graph.

absorption edge and emission peak. This is due to the non-radiative decay of some electrons from the conduction band of the host material to the defect states before their radiative decay.

3.2. Time-resolved luminescence

3.2.1. Time-resolved luminescence of CdS:Te QDs. In order to further investigate the luminescence mechanism of CdS QDs doped with Te and determine the cause of the shift of emission peak, time-resolved luminescence was measured and analyzed. Figure 3(a) shows transient luminescence dynamics for a few different emission photon energies for CdS:Te:1.1% QDs. It is seen that the intensity of higher-energy photons decays more rapidly than that of lower-energy photons. Consequently, the emission peak shifts from 2.03 to 1.84 eV during the transient emission process, as shown in figure 3(b). After 130 ns, the emission peak does not shift anymore. The underlying mechanisms will be explained in the subsequent sections.

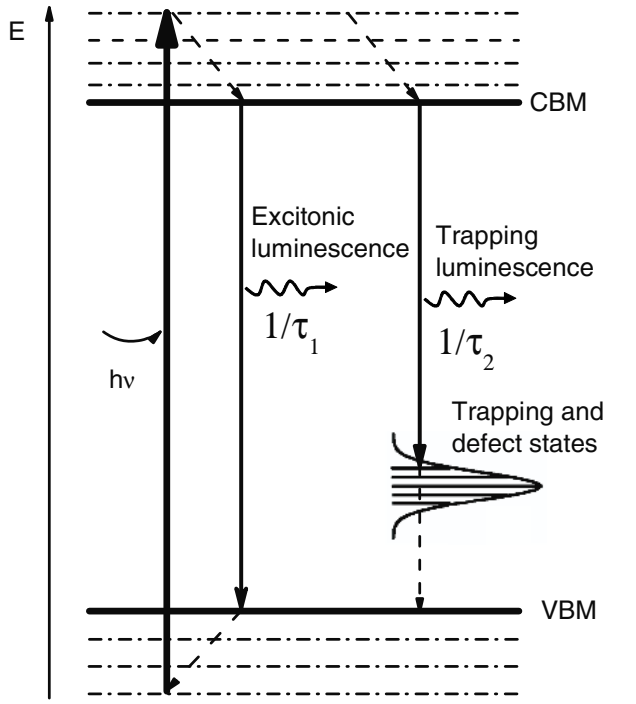

Figure 4. Energy level diagram of CdS:Te QDs, where trapping and defect states are shown. CBM, conduction band minimum; VBM, valance band maximum.

3.2.2. Decomposition of luminescence spectra and the energy level model. The emission peak shift indicates that different emission mechanisms with different dynamics may exist concurrently. To quantitatively analyze the transient emission spectra, we treat the time-resolved spectra at different delay times as a matrix in the singular value decomposition (SVD) analysis, which has been widely used to analyze transient absorption spectra [17]. The measured spectra in the spectral range 1.28–2.84 eV (1024 channels) at delay times from −35 to 700 ns are processed by SVD to determine the minimum number of basis spectrum sets to describe the data. After SVD, the data matrix could be approximately expressed as

$$A = \sum_i s_i V_i t_i^T, \tag{1}$$

where s_i, t_i and V_i are the spectrum, temporal evolution and singular weight value of the ith SVD component, respectively. For all the three CdSTe QD samples, we find $V_1 - V_2 \gg V_3$ in SVD analysis, indicating that the spectrum contains two major components. Therefore, we fit each decay curve with a biexponential function, as shown in the inset of figure 3(a). One component decays rapidly and the other decays much more slowly, indicating that they come from excited states of different natures. Considering the red shift of the emission peak with time, we conclude that the lower-energy component in the spectrum comes from the more slowly decaying state.

These two emission channels with different lifetimes can be explained using a three-level energy diagram model shown in figure 4. The bandgap of the Te doped CdS QD is significantly lower than that of the base CdS QD, and the band-edge emission is denoted as 'excitonic luminescence' with a

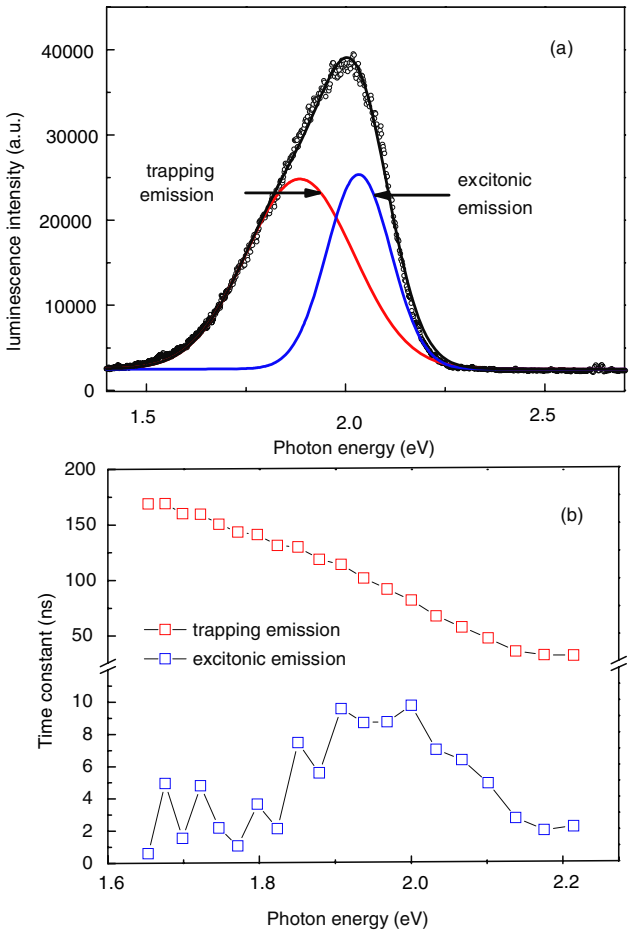

Figure 5. (a) The luminescence spectrum of CdS:Te QDs with a Te/S molar ratio of 1.1%. It can be decomposed into a higher-energy component (blue) due to excitonic emission and a lower-energy component due to trapping state emission (red). (b) Lifetime of the excitonic and trapping state emissions as a function of photon energy.

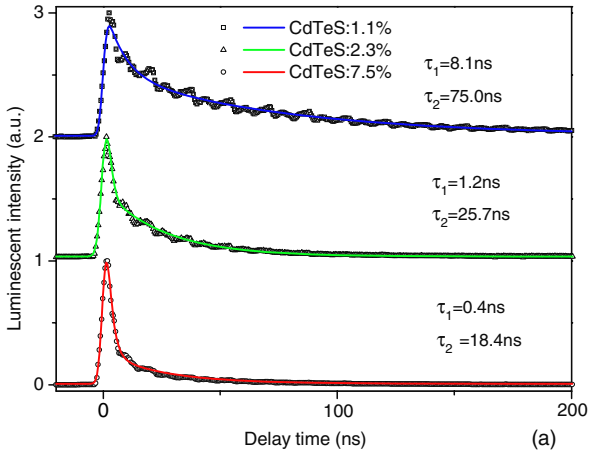

Figure 6. Normalized luminescence decay curves of three CdS:Te QD samples at 400 nm laser excitation. The decays of three different CdS:Te QDs are integrated about 30 nm near the emission peak.

lifetime τ_1. In addition, trapping or defect states appear within the bandgap with a lifetime τ_2. For a bulk semiconductor these trapping levels are inactive because of optical transition is forbidden. However, in QDs, especially under intense femtosecond laser excitation, transitions between these energy levels become allowed. A defect-related or trapping state is commonly observed in II–VI semiconductor QDs [18], and a broad emission band [19] or a long tail [20] has been reported and attributed to trapping states. Similar electronic structures have been reported in Cu doped ZnSe [8] and Mn doped CdS [9].

During the photoluminescence process, the electrons are first excited from the valence band to the conduction band states higher than the conduction band minimum (CBM). These hot electrons rapidly decay to the CBM through electron–phonon scattering processes [3]. Then the electrons recombine with holes on the valence band maximum (VBM) of the host quantum dots by emitting photons. The electrons can also recombine with holes located at trapping states near the VBM. Therefore, the emission spectra of doped CdS QDs consist of excitonic and impurity state emissions. Photons from the trapping state emission have a slightly lower energy than those from the excitonic state emission, but they are often indistinguishable in the total emission spectra when broadening is considered [21]. Figure 5(a) shows the decomposition of the two emission mechanisms, each having a Gaussian profile. Figure 5(b) shows the lifetime for each channel as a function of the photon energy. The lifetime of the band-edge excitonic emission is of the order of 10 ns and is not strongly dependent on wavelength, while the lifetime of the trapping state [22] varies significantly from 32.9 to 169.0 ns for photon energies from 2.20 to 1.65 eV.

3.2.3. Composition dependence of the photoluminescence. The decay dynamics of three different QD samples under 400 nm laser excitation are shown in figure 6, where τ_1 and τ_2 are the average lifetimes for the excitonic and trapping states, respectively. The total lifetime τ_{av} is obtained using the equation [23, 24]

$$\tau_{av} = \frac{a_1\tau_1 + a_2\tau_2}{a_1 + a_2} \tag{2}$$

where a_1 and a_2 denote the amplitude of band-edge excitonic and trapping state emissions, respectively. Figure 6 shows that the total lifetime τ_{av} decreases from 39.5 to 2.6 ns when increasing the Te concentration from 1.1% to 7.5%. This trend is opposite to that found when increasing the size of QDs, though both Te doping and larger size can lead to a red shift in the emission peak. The hole wavefunction is spatially localized around the Te impurity. With the Te concentration increasing, the hole wavefunction has a higher overlap with the electron wavefunction, and more trapping states within the energy gap can be formed. Therefore, electron–hole recombination becomes more efficient and the lifetime is shorter. Non-radiative recombination can become more efficient when the Te doping concentration increases, which further shortens the electron lifetime. Similar arguments have been made in other doped systems where higher doping concentration enhances energy transfer and self-quenching rates so as to shorten the electron lifetimes [25, 26].

4. Conclusions

In summary, a series of CdS:Te QDs at different doping levels are synthesized using the one-step organometallic method, and steady-state and time-resolved luminescence spectra are measured and analyzed. We observe that the transient emission spectra of the three doped QDs have an evident red shift of the emission peak with time. We decompose the luminescence to band-edge excitonic emission and trapping state emission using singular value decomposition and multiexponential fitting. Results show a shortened lifetime for higher Te concentration which may originate from higher overlap between the electron and hole wavefunctions, a higher density of defect energy levels and stronger nonradiative recombination.

Acknowledgments

This work was partially supported by the National Science Foundation (grant no. CTS-0933559). Wu and Zheng also acknowledge the partial financial support of the Key Laboratory of Electronics Engineering, College of Heilongjiang Province. Helpful discussions and proofreading by Hua Bao and Liangliang Chen are appreciated.

References

[1] Chan W C W and Nie S M 1998 *Science* **281** 2016–8
[2] Sun Q J, Wang Y A, Li L S, Wang D Y, Zhu T, Xu J, Yang C H and Li Y F 2007 *Nat. Photon.* **1** 717–22
[3] Bao H, Habenicht B F, Prezhdo O V and Ruan X L 2009 *Phys. Rev.* B **79** 235306
[4] Peng Z A and Peng X G 2001 *J. Am. Chem. Soc.* **123** 183–4
[5] Zhong X H, Feng Y Y, Knoll W and Han M Y 2003 *J. Am. Chem. Soc.* **125** 13559–63
[6] Rogach A L, Thomas F, Klar T A, Feldmann J, Gaponik N, Lesnyak V, Shavel A, Eychmüller A, Rakovich Y P and Donegan J F 2007 *J. Phys. Chem.* C **111** 14628–37
[7] Ou yang J Y, Ratcliffe C I, Kingston D, Wilkinson B, Kuijper J, Wu X H, Ripmeester J A and Yu K 2008 *J. Phys. Chem.* C **112** 4908–19
[8] Xing G C, Ji W, Zheng Y G and Ying J Y 2008 *Opt. Express* **16** 5715–20
[9] Gan C L, Zhang Y P, Battaglia D, Peng X G and Xiao M 2008 *Appl. Phys. Lett.* **92** 241111
[10] Nemec P and Maly P 2000 *J. Appl. Phys.* **87** 3342–8
[11] Tomihira K, Kim D G and Nakayama M 2005 *J. Lumin.* **112** 131–5
[12] Stouwdam J W and Janssen R A J 2009 *Adv. Mater.* **21** 2916–20
[13] Bhargava R N 1996 *J. Lumin.* **70** 85–94
[14] Franzl T, Müller J, Klar T A, Rogach A L, Feldmann J, Talapin D V and Weller H 2007 *J. Phys. Chem.* C **111** 2974–9
[15] Morello G, Anni M, Cozzoli P D, Manna L, Cingolani R and De Giorgi M 2007 *J. Phys. Chem.* C **111** 10541–45
[16] Peng X G, Manna L, Yang W D, Wickham J, Scher E, Kadavanich A and Alivisatos A P 2000 *Nature* **404** 59–61
[17] Zhang J P, Inaba T, Watanabe Y and Koyama Y 2000 *Chem. Phys. Lett.* **331** 154–62
[18] Wuister S F, van Driel F and Meijerink A 2003 *Phys. Chem. Chem. Phys.* **5** 1253–8
[19] Chen W, Joly A G and McCready D E 2005 *J. Chem. Phys.* **122** 224708
[20] Kapitonov A M, Stupak A P, Gaponenko S V, Petrov E P, Rogach A L and Eychmuller A 1999 *J. Phys. Chem.* B **103** 10109–13
[21] Poles E, Selmarten D C, Micic O I and Nozik A J 1999 *Appl. Phys. Lett.* **75** 971–3
[22] Wang X Y, Qu L H, Zhang J, Peng X G and Xiao M 2003 *Nano Lett.* **3** 1103–6
[23] Li J and Xia J 2000 *Phys. Rev.* B **62** 12613–6
[24] Biju V, Kanemoto R, Matsumoto Y, Ishii S, Nakanishi S, Itoh T, Baba Y and Ishikawa M 2007 *J. Phys. Chem.* C **111** 7924–32
[25] Ruan X L and Kaviany M 2005 *J. Appl. Phys.* **97** 104331
[26] Ruan X L and Kaviany M 2006 *Phys. Rev.* B **73** 155422